SENSITIVITY EVALUATION OF GAS-PHASE REDUCTION MECHANISMS OF DIVALENT MERCURY USING CMAQ-HG IN A CONTIGUOUS US DOMAIN

Pruek Pongprueksa* and Che-Jen Lin
Department of Civil Engineering, Lamar University, Beaumont, TX, USA

Thomas C. Ho
Department of Chemical Engineering, Lamar University, Beaumont, TX, USA

1. INTRODUCTION

The chemical mechanism of atmospheric mercury implemented in the current release of CMAQ-Hg (V.4.5.1) includes the gas-phase oxidation and aqueous phase oxidation/reduction. However, the uncertainty of the chemical scheme has been reported in earlier studies (Calvert and Lindberg 2005, Gårdfeldt and Jonsson 2003, and Lin *et al.* 2006). Although there has not been deterministic kinetic and mechanistic study of the reduction of divalent mercury in the gaseous phase, there were a few earlier investigations showing the potential reduction of divalent mercury by reducing species relevant to the atmospheric chemistry of mercury. These reactions include the photolysis or photo-dissociation of mercuric oxide (HgO) and gas-phase reduction of HgO by carbon monoxide (CO), Fay and Seeker (1903). In this study, we performed sensitivity analyses using CMAQ-Hg by implementing the two reduction mechanisms in CMAQ-Hg. We attempted to test if such reduction implementation in CMAQ-Hg would improve the model performance when compared to the field measurements of mercury deposition.

2. APPROACH

A series of sensitivity simulations using various reduction rate constants of HgO by photoreduction and HgO reduction by CO are conducted to project the kinetic parameters to be employed in the model using a modified version of CMAQ-Hg 4.5.1. The model performance is assessed based on the verification with the wet deposition data reported by the Mercury Deposition Network (MDN). The simulations are performed for the entire month of July 2001 in a 36-km Lambert conformal Contiguous Unites States (CONUS) domain with USEPA's 2001 gridded emission inventory and MM5 meteorology data. The aqueous reduction of divalent mercury by $HO_2^{\bullet}$ is turned off, and the gas-phase mercury oxidation products by $OH^{\bullet}$ and O_3 are assigned to be 100% Hg(II) in the simulations. We report the model response to the reduction mechanism implementation herein. The model results are interpreted in terms of the uncertainty of mercury chemical mechanism and the possibility of gas-phase reduction of divalent mercury in the atmosphere. The feasible magnitude of the kinetic parameters of the reduction pathways of mercury is also discussed.

2.1 CMAQ-Hg Model Input Data

Meteorological data - 2001 The PSU/NCAR mesoscale model (MM5) and the meteorology-chemistry interface processor (MCIP) version 3.1 with M3Dry dry deposition velocity for mercury species calculation.

Emission inventory – the United States and Canada anthropogenic mercury emissions based on 1999 NEI emissions inventory and vegetative mercury emission inventory reported by Lin *et al.* (2005).

Initial and boundary conditions – default profile files embedded in the CMAQ-Hg model [1.73-1.78 x 10^{-7} ppmV for Hg(0), 2.0-7.0 x 10^{-9} ppmV for Hg(II)gas, and 1.62-10.80 x 10^{-6} μg m^{-3} for Hg(P)].

2.2 CMAQ-Hg Model Configuration

Hg oxidation products – the Hg oxidation products distribution has been experimented extensively in CMAQ-Hg versions including in this study. The previous CMAQ-Hg described by Bullock and Brehme (2002) speciate the products from Hg(0) by O_3, H_2O_2, and OH reactions to be all particulate form of mercury or Hg(P). According to Lin and Tao (2003) and the official release of CMAQ 4.5.1, the updates in mercury chemistry

---

**Corresponding author:* Pruek Pongprueksa, Air Quality Modeling Laboratory, C2609, Department of Civil Engineering, Lamar University, Beaumont, TX 77710; phone: (409) 880-8708, e-mail: ppongpruek@my.lamar.edu

are as follows: (1) gaseous elemental mercury (GEM) oxidation by hydrogen peroxide is assumed to produce 100% divalent gaseous mercury; (2) GEM oxidation by ozone is assumed to produce 50% divalent gaseous mercury and 50% aerosol mercury; (3) GEM oxidation by hydroxyl radical is assumed to produce 50% divalent gaseous mercury and 50% aerosol mercury. In this study, we assigned the products from Hg(0) oxidation reactions with O_3, H_2O_2, and OH to be all gaseous divalent mercury or Hg(II). The products distribution comparison for the CMAQ versions is shown in Fig. 1.

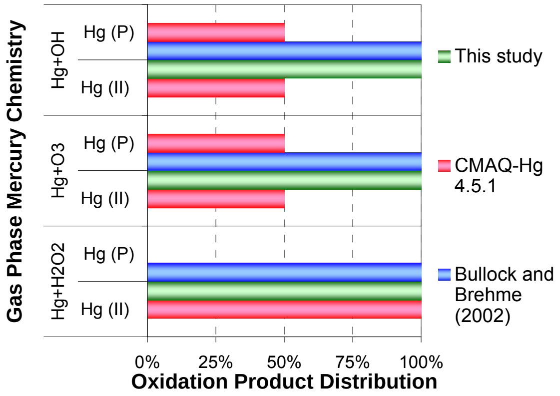

Fig. 1. Gaseous mercury oxidation products distribution in various CMAQ-Hg versions

Hg reduction mechanism by CO – Bullock and Brehme (2002) suggested that chemical reduction of Hg(II) to Hg(0) might occur in the gas phase but the mechanism and rate for this type of reaction remains uncertain. The reduction mechanism proposed in this study is based on Fay and Seeker (1903) experiment that showed the lowest experimental reduction temperature of mercury oxides by carbon monoxide as low as 0°C for mercurous oxide and mercuric oxide (yellow). The reduction mechanism is believed to be

$$HgO(s,g) + CO(g) \xrightarrow{k1} Hg(g) + CO_2(g) \qquad (1)$$

where k_1 is the reduction rate of the reaction. This reaction is an exothermic reaction which a reaction enthalpy of -130.7 kJ mol^{-1}. In this study, we selected reaction rate ranging from 10^{-20} to 10^{-14} cm^3 $molecule^{-1}$ s^{-1} for the sensitivity evaluation.

Hg photoreduction mechanism – this reduction mechanism relies on the property of mercuric oxide (HgO), which will be degraded when exposes to sunlight. The photoreduction mechanism of HgO can be written as

$$HgO(s,g) + hv \xrightarrow{J(HgO)} Hg(g) + \frac{1}{2}O_2(g) \qquad (2)$$

and

$$J(HgO) = f \times J(NO_2) \qquad (3)$$

where J(HgO) is photoreduction rate coefficient of HgO, $J(NO_2)$ is photolysis rate coefficient of NO_2 ($\approx 8.82 \times 10^{-3}$ s^{-1} at ground level, Jacobson 1999), f is multiply factor to $J(NO_2)$ for J(HgO) estimation. For this reduction mechanism, we chose the factor ranging from 10^{-5} to 10^{1} for the sensitivity evaluation.

2.3 CMAQ-Hg Model Evaluation

CMAQ-Hg is a useful model for study of atmospheric mercury (chemistry transformation and transport). The model can simulate mercury species in terms of concentration, dry and wet deposition in the atmosphere. However, there is inadequate field measurement for model evaluation, mainly for mercury concentration and dry deposition in the study area. The available data are total mercury wet deposition operated by mercury deposition network (MDN). The data from MDN contain national database of weekly concentrations of total mercury in precipitation and the seasonal and annual flux of total mercury in wet deposition. However, the data (precipitation and wet deposition) from simulation and observation have a degree of discrepancy. In order to reduce inconsistency, we selected sites for data comparison that contain MCIP precipitation data within the multiply factor of 0.5-2.0 of MDN precipitation data (see Fig. 2.).

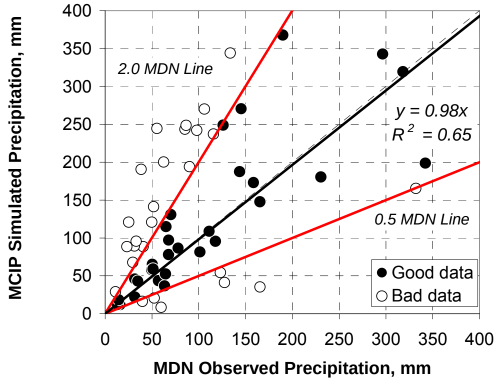

Fig. 2. Monthly (July 2001) precipitation comparison of MCIP simulated data vs. MDN observed data

After the comparable sites are selected, we normalized the simulated wet deposition data using the observed precipitation data for model performance evaluation.

3. RESULTS AND DISCUSSION

Fig. 3 shows the simulated total Hg wet deposition flux in July 2001 by using CMAQ-Hg 4.5.1. The results are lower estimated as 44% lower than that of the selected MDN monitoring stations (~ 0.56 MDN). The spatial distribution of total Hg wet deposition is related to the distribution of precipitation from MCIP. The deposition becomes much enhanced when aqueous HO_2 reduction of $Hg(II)_{aq}$ is turned off and all Hg oxidation products is assigned as $Hg(II)_g$ as shown in Fig. 4. The wet deposition result is increased by 275% compared to the original model result (increase from 0.56 to 1.54 MDN measured wet depositions). Therefore the controversial aqueous reduction by HO_2 is the most influential reduction mechanism in the current model treatment.

We tested two conceivable reduction mechanisms in gaseous phase chemistry (reduction by CO and HgO photoreduction). For the CO reduction, we found that a reduction rate constant of 5×10^{-18} cm^3 $molecule^{-1}$ s^{-1} gives wet deposition data comparable to the MDN ones (0.97 MDN measured wet deposition, $r^2 = 0.78$, see Fig. 5). By trial-and-error method, we found that a HgO photoreduction rate of 8.82×10^{-6} s^{-1} produced a simulated wet Hg deposition compared favorably to MDN data (1.04 MDN measured wet deposition, $r^2 = 0.72$, see Fig. 6).

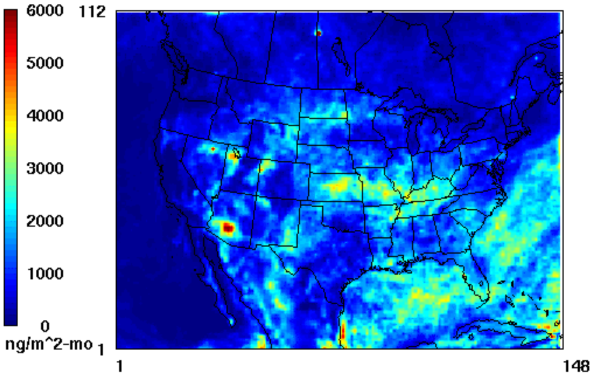

Fig. 3. Simulated total Hg wet deposition flux in July 2001 from official release version of CMAQ-Hg 4.5.1

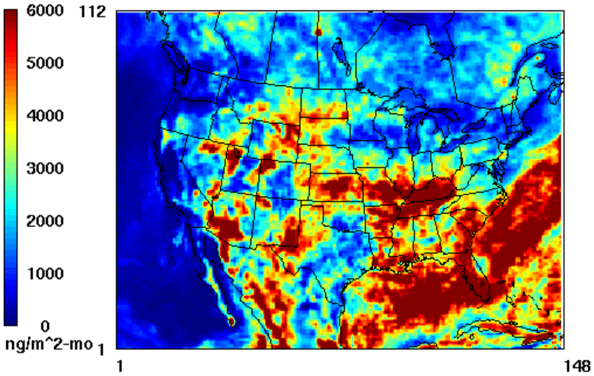

Fig. 4. Simulated total Hg wet deposition flux in July 2001 from a modified CMAQ-Hg 4.5.1 (oxidation products are Hg(II) and no HO_2 reduction)

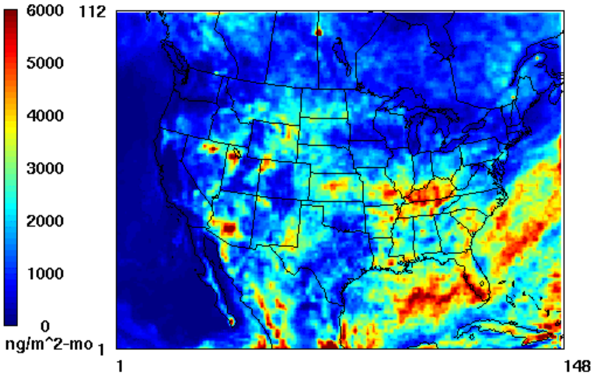

Fig. 5. Simulated total Hg wet deposition flux in July 2001 by CO reduction mechanism ($k = 5 \times 10^{-18}$ cm^3 $molecule^{-1}$ s^{-1})

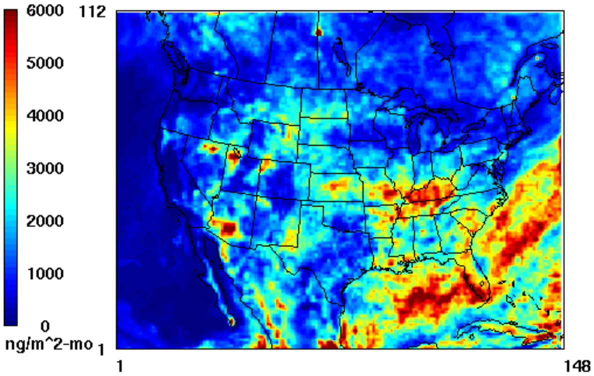

Fig. 6. Simulated total Hg wet deposition flux in July 2001 by photoreduction mechanism ($J_{Hg(II)} = 10^{-3} J_{NO2} \approx 8.82 \times 10^{-6}$ s^{-1})

In addition, we varied the reduction rates from 10^{-20} to 10^{-14} cm^3 $molecule^{-1}$ s^{-1} by CO and the Hg photoreduction rates from 8.82×10^{-8} to 8.82×10^{-2} s^{-1}. Then, we plotted the simulated Hg wet deposition fluxes against the MDN data to find the relationship between the simulated and measured wet deposition (Fig 7 & 8).

Fig. 7 shows log-log graph of total Hg wet deposition comparisons between MDN and CMAQ. We varied CO reduction rates in CMAQ simulation and plotted MDN observed wet deposition data (x-axis) against CMAQ simulated data (y-axis) in July 2001. For Fig. 8, we varied photoreduction rates in CMAQ model and plotted MDN observed results against CMAQ simulated results. The relationships obtained from these graphs were then used to construct Fig. 9.

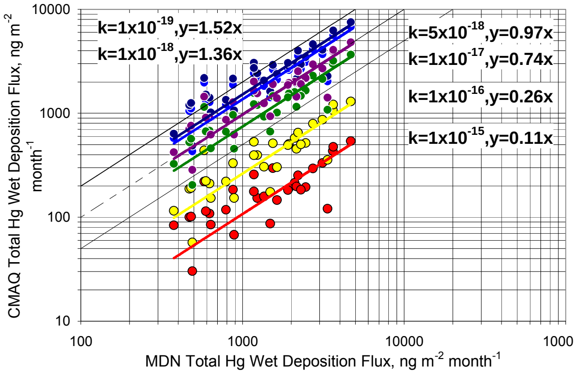

Fig. 7. Total Hg wet deposition comparison MDN vs. CMAQ by varying CO reduction rate, July 2001

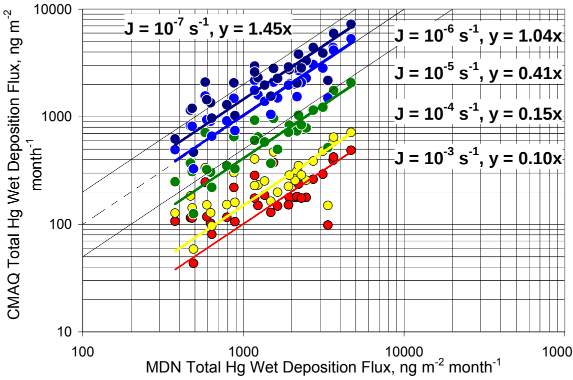

Fig. 8. Total Hg wet deposition comparison MDN vs. CMAQ by varying photoreduction rate, July 2001

Fig. 9 shows the minimum, optimum, and maximum rates based on our sensitivity simulations. The minimum rate is the rate that, when implemented to the model, shows insignificant impact to total Hg wet deposition flux. From the study, we found that the minimum rates for CO reduction and photoreduction are 1 x 10^{-20} cm^{3} molecule^{-1} s^{-1} and 1 x 10^{-7} s^{-1}, respectively. The optimum rate is the rate that produces most favorable to measured wet deposition by MDN. We found that the optimum rates for CO reduction and photoreduction are 5 x 10^{-18} cm^{3} molecule^{-1} s^{-1} and 1 x 10^{-5} s^{-1}, respectively. The maximum rates for CO reduction and photoreduction are 1 x 10^{-15} cm^{3} molecule^{-1} s^{-1} and 1 x 10^{-2} s^{-1}, respectively, greater than which the increase of the rate constant does not affect simulated wet deposition. The maximum rates can also be used to suggest the upper limit of the model simulation and the laboratory experiment.

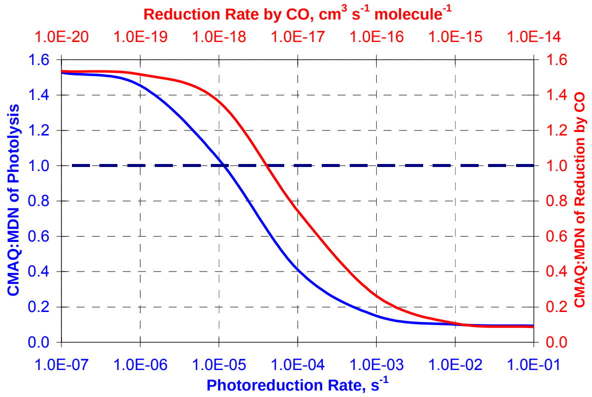

Fig. 9. Total Hg wet deposition flux influenced from Hg(II) reduction by photoreduction (blue line) and CO reduction reaction (red line)

A combination of the two reduction mechanisms can also generate the similar wet deposition result presented here. The range of the reduction rates between minimum and optimum from both mechanisms can be randomly tried. However, we need to further examine and evaluate with the laboratory testing.

4. SUMMARY

We conducted a series of sensitivity simulations using various reduction rate constants of Hg(II) by photoreduction and Hg(II) reduction by CO to demonstrate the kinetic parameters to be employed in the model using a modified version of CMAQ-Hg 4.5.1. We reported the model response to the reduction mechanisms when the aqueous reduction of divalent mercury by $HO_2^{\bullet}$ is turned off, and the gas-phase mercury oxidation products by $OH^{\bullet}$ and O_3 are assigned to be 100% Hg(II). From the study, the minimum rates for CO reduction and photoreduction are 1 x 10^{-20} cm^{3} molecule^{-1} s^{-1} and 1 x 10^{-7} s^{-1}, respectively. These two reduction mechanisms will be insignificant when the reduction rate from the laboratory experiment is less than the minimum value. In this study, we found that the optimum rates for CO reduction and photoreduction are 5×10^{-18} cm^3 $molecule^{-1}$ s^{-1} and 1×10^{-5} s^{-1}, respectively. However, these rate constants provide a preliminary estimate for further verification by more kinetic laboratory studies.

5. ACKNOWLEDGMENTS

The study is supported in part by the US Environmental Protection Agency (USEPA, RTI subcontract No. 3-93U-9606) and Texas Commission on Environmental Quality (TCEQ work order No. 64582-06-15). The funding support is gratefully acknowledged.

6. REFERENCES

Calvert, J. G., and S. E. Lindberg, 2005: Mechanisms of mercury removal by O_3 and OH in the atmosphere. *Atmospheric Environment*, **39,** 3355–3367.

Gårdfeldt, K., and M. Jonsson, 2003: Is bimolecular reduction of Hg(II) complexes possible in aqueous systems of environmental importance. *J. Phys. Chem. A,* **107,** 4478-4482.

Lin, C. J., P. Pongprueksa, S. E. Lindberg, S. O. Pehkonen, D. W. Byun, and C. Jang, 2006: Scientific uncertainties in atmospheric mercury models I: model science evaluation. *Atmospheric Environment*, **40,** 2911–2928.

Fay, I. W., and A. F. Seeker, 1903: Reducibility of some metallic oxides by hydrogen and carbon monoxide. *J. Am. Chem. Soc.*, **25**(6), 641-647.

Lin, C. J., S. E. Lindberg, T. C. Ho, and C. Jang, 2005: Development of a processor in BEIS3 for estimating vegetative mercury emission in the continental united states. *Atmospheric Environment*, **39,** 7529–7540.

Bullock, O. R., and K. A. Brehme, 2002: Atmospheric mercury simulation using the CMAQ model: formulation description and analysis of wet deposition results. *Atmospheric Environment,* **36,** 2135-2146.

Lin, X., and Y. Tao, 2003: A numerical modelling study on regional mercury budget for eastern north america. *Atmos. Chem. Phys.*, **3,** 535–548.

Jacobson, M. Z., 1999: *Fundamentals of Atmospheric Modeling*. Cambridge University Press, 672 pp.